Article:
Bai, L, Zhang, L, Lin, G et al. (2 more authors) (2015) Development of cryogenic loop heat pipes: A review and comparative analysis. Applied Thermal Engineering, 89. pp. 180-191. ISSN 1873-5606

https://doi.org/10.1016/j.applthermaleng.2015.06.010

Development of cryogenic loop heat pipes: a review and comparative analysis

Lizhan Bai[1,*], Jinghui Guo[1], Guiping Lin[1], Jiang He[2], Dongsheng Wen[3]

1 Laboratory of Fundamental Science on Ergonomics and Environmental Control, School of Aeronautic Science and Engineering, Beihang University, Beijing 100191, PR China

2 Beijing Key Laboratory of Space Thermal Control Technology, Beijing Institute of Spacecraft System Engineering, Beijing 100094, PR China

3 School of Chemical and Process Engineering, University of Leeds, Leeds, LS2 9JT, UK

Abstract: Loop heat pipes(LHP) are highly efficient two-phase heat transfer devices with the ability to transfer a large amount of heat over a long distance. Due to increasing demand of efficient cryocooling applications in both space and terrestrial surroundings, LHPs operating in cryogenic temperature range have been extensively investigated in recent years. This work provided a comprehensive review of state-of-art cryogenic loop heat pipes (CLHPs) Five different types of CLHP were categorized, and a comparative analysis between CLHPs and ambient LHPs and among different types of CLHPs were conducted. The operation and performance characteristics of different types of CLHPs were compared in terms of the system structure, supercritical startup, heat transport capacity and the effect of parasitic heat load. The parameters that affect the CLHP performance were analyzed and the optimization strategy was presented in order to progress their future development and applications .

Keywords: loop heat pipe; cryogenic; supercritical startup; heat transport

* Corresponding author. Tel.: +86 10 8233 8600; fax: +86 10 8233 8600.
E-mail address: bailizhan@buaa.edu.cn (L. Bai).

1 Introduction

Loop heat pipes (LHPs) are highly efficient two-phase heat transfer devices that utilize the evaporation and condensation of a working fluid to transfer heat, and capillary forces developed in fine porous wick to circulate the working fluid[1, 2]. Compared with traditional heat pipes, LHPs have the advantage of transferring a larger amount of heat over a longer distance with strong antigravity capability. Moreover, the arrangement of LHP to connect the heat source and heat sink becomes more convenient due to its flexible transport lines.

A typical LHP is composed of an evaporator, a condenser, a compensation chamber (CC) and vapor and liquid transport lines. Fig.1 shows the detailed structure of the evaporator and CC, and Fig.2 shows the schematic view of a typical LHP. The vapor transport line connects the vapor grooves and the condenser inlet, and the liquid transport line connects the bayonet extending to the evaporator core and the condenser outlet. The basic working principle and operating characteristics of an LHP were introduced in Ref.[2]. When heat load is applied to the evaporator, liquid is vaporized at the outer surface of the evaporator wick, and the menisci formed in the evaporator wick develop a capillary pressure to push the vapor collected in the vapor grooves through the vapor transport line to the condenser, where the fluid condenses and the heat is rejected to the heat sink. The condensed liquid is pushed back through the liquid transport line to the evaporator core, which provides liquid replenishment to the evaporator wick to complete the circulation. As the capillary forces developed in the evaporator wick is the driving source for the circulation of the working fluid along the loop, no external power is needed in the operation of an LHP.

The development of LHPs was originated in 1972 by the Russian scientists Gerasimov and Maydanik from the Ural Polytechnical Institute. The first LHP had a transport length of 1.2m and heat transfer capacity of about 1kW using water as the working fluid. [ref[The first space flight experiment was

conducted in 1989 aboard the Russian spacecraft “Gorizont”, which demonstrated the serviceability of LHP in reduced gravity conditions [1]. Since their initial conceptualization, these devices have attracted considerable interests from researchers worldwide including USA, Canada, China, Japan, Brazil, French and Australia to develop better space thermal control systems Both experimental and theoretical work have been conducted, which confirmed that LHPs poesessed good self-startup capability, excellent heat transfer performance and strong antigravity capability [3-9]. To date, more than one hundred LHPs with cylindrical evaporators have been applied in the thermal control systems of many spacecraft, and the number still keeps increasing.

With the rapid development of LHP technology for space applications, its application has been extended to terrestrial surroundings, such as in the thermal management of aircraft and submarines, and the cooling of high power-density electronic devices[10-20]. Since most of the heat sources or objects to be cooled have flat thermo-contact surfaces, LHPs with flat evaporators including both opposite liquid replenishment and longitudinal liquid replenishment have been developed and tested extensively. It is found that a LHP with stainless steel-nickel-ammonia combination is the most efficient for temperature range at 40-70℃, while the copper-copper-water combination performs best at 70-100℃ range[21].

LHPs mentioned above are are termed as ambient loop heat pipes (ALHPs) as they are operating within the ambient temperature range; and the working fluids are typically ammonia, water, acetone or methanol, etc. They are not suitable for cryogenic temperature applications. For instance the thermal control of a space infrared exploration system requires maintaining the infrared sensors/detectors at 80-100K, and the cooling of superconducting magnet and small-scale particle detectors on the ground requires even lower temperature. LHPs operating in the cryogenic temperature range, termed as cryogenic loop heat pipes (CLHPs), must be developed and investigated systematically.

The development of CLHP was initiated at the beginning of this century, and considerable achievement has been obtained . CLHPs with different system structures and operation temperatures have been developed and investigated both experimentally and theoretically. These devices have been reported to start successfully at supercritical conditions and operate steadily in the corresponding cryogenic temperature range. They can be applied in both space and terrestrial surroundings, and the lowest operating temperature range has been extended to 3-5K. In addition, these devices could provide efficient cryocooling of both concentrated and large area heat sources.

In this paper, the development of cryogenic loop heat pipes (CLHPs) will be reviewed in detail, and the operating principle and characteristics as well as the application fields of each type of CLHP will be comparatively analyzed. This will form understanding of the principal differences among different types of CLHPs and provide guidance to the design and application of these devices.

2 Cryogenic working fluids

As CLHPs are operating in the cryogenic temperature range, appropriate cryogenic working fluids must be selected first The available cryogenic working fluids for selection is actually quite limited, and as a rule of thumb : propane for the operating temperature range of 200-240K, oxygen for 90-140K, nitrogen for 80-110K, neon for 30-40K, hydrogen for 20-30K. When the operating temperature is further reduced to 2-4K, helium will be an appropriate cryogenic working fluid.

The cryogenic working fluids charged into the system determine the operating temperature range, heat transfer performance, heat transport capacity and the lifespan of the CLHPs. Compared with ambient working fluids such as ammonia and water, cryogenic working fluids have much smaller surface tension and evaporative latent heat, hence much lower Dunbar Parameter, as defined below :

$$\mathrm{Du} = \frac{\lambda^{1.75}\sigma\rho_{\mathrm{v}}}{\mu_{\mathrm{v}}^{0.25}} \tag{1}$$

Based on the evaluation of the capillary limit, which takes comprehensive thermo-physical properties of the working fluid into account, a higher Dunbar Parameter will produce a larger heat transport capacity of the LHP charged with that working fluid.

Fig.3 shows the variation of Dunbar Parameter of ambient working fluids, i.e. ammonia and water, and Fig.4 shows the variation of Dunbar Parameter of cryogenic working fluids including nitrogen, argon, oxygen, hydrogen and helium. Comparing Fig.4 with Fig.3, the maximum Dunbar Parameter for ammonia reaches above $160\times10^{9}W^{1.75}$ at 50℃, and a higher number is seen for water at a temperature > 130℃. However the maximum Dunbar Parameters for nitrogen, argon and oxygen are $3.2\times10^{9}W^{1.75}$, $4.4\times10^{9}W^{1.75}$ and $6.3\times10^{9}W^{1.75}$ respectively, and it is reduced to $2.3\times10^{6}W^{1.75}$ for helium. It is evident that the cryogenic working fluids have much lower Dunbar Parameter, which will result in reduced heat transport capacity of CLHPs comparing to ALHPs. This issue must be carefully considered in the design of CLHPs.

3 Cryogenic loop heat pipes with different types

To date, several types of CLHPs have been developed and investigated both experimentally and theoretically to satisfy different applications at varying operation temperatures. Five types are summarized based on the difference of system structure and layout, as reviewed in detail below.

3.1 Type A

3.1.1 System structure

Fig.5 shows the schematics of this type of CLHP, which is composed of an evaporator, a condenser, a CC and vapor and liquid transport lines plus a gas reservoir. Compared with an ALHP, the type of CLHP

only has one additional gas reservoir, which has the simplest structure among all types of CLHPs.

3.1.2 Supercritical startup

For type A CLHP to realize a supercritical startup, the gravity-assisted method has been proposed. The gravity-assisted method is to utilize gravity to cool and saturate the evaporator wick of the CLHP without using any additional components. For type A CLHP, the condenser must be placed higher than the evaporator during the supercritical startup. A typical startup process is as follows: Prior to the startup, the whole CLHP is at the ambient state, and the condenser temperature begins to decrease as the cryogenic heat sink takes effect. Condensation occurs after reaching th local saturation temperature, and the condensate flow into the evaporator through both the liquid and vapor transport lines due to the effect of gravity. Once the evaporator wick is fully saturated with liquid, heat load can be applied to the evaporator to start up the CLHP.

3.1.3 Experimental results

Only very limited work was reported for type A CLHP. Pereira et al.[22] constructed and experimentally investigated a CLHP as a potential candidate for the cooling of small-scale particle detectors. Noble gases and propane were selected as the cryogenic working fluids. The outer diameter and length of the cylindrical evaporator were 18 and 30mm respectively, and the transport distance was 350mm. The condenser and the liquid and vapor transport lines were all 4mm inner diameter tubes. Both the evaporator and condenser were made of copper to ensure good thermal conduction between the heat sink and heat source. The CC and the transport lines were made of stainless steel. The heat sink was provided by an commercial Gifford-McMahon cryocooler. Experimental results showed that the CLHP could easily realize the supercritical startup by using the gravity-assisted method without any other auxiliary measures. There was

an optimal working fluid inventory for each cryogenic working fluid to achieve the best heat transfer performance. The heat transport capacity of the CLHP was 20W for argon as the cryogen fluid, and it increased to 25W and 30W for krypton and propane respectively. Comparing with the gravity-assisted mode, the operation temperature was much higher when the condenser was nearly level with the evaporator. r.

3.2 Type B

3.2.1 System structure

Fig.6 shows the schematic of this type of CLHP. Compared with an ALHP, the CLHP has an additional secondary evaporator in addition to the gas reservoir. The secondary evaporator is attached directly to the cryogenic heat sink and is connected in series with the condenser line, which separates the condenser line into two parts. The secondary evaporator is typically like the evaporation section of a traditional grooved heat pipe, and the wick is made of axial grooves machined directly on the inner surface of the pipe wall.

3.2.2 Supercritical startup

The use of a secondary evaporator, type B, is mainly for the consideration of supercritical startup. A typical startup process is similar to type A except that additional heat is applied on the secondary evaporator. The produced vapor push the condensate into the primary evaporator and CC through the liquid and vapor transport lines. Until the wick is fully saturated with the liquid, heat load is applied to the primary evaporator to start up the CLHP. As the vapor has no preferable direction to push the condensate, it cannot establish one-way circulation of the working fluid in the loop. The application of heat load to the secondary evaporator therefore should be intermittent.

3.2.3 Experimental results

Within this category, Mo et al.[23-25] designed and experimentally investigated a nitrogen-charged CLHP. The outer diameter and length of the primary evaporator were 20 and 100mm respectively, and the transport distance was about 170mm. The heat sink was provided by a copper plate cooled by liquid nitrogen. Experimental results showed that the whole CLHP could be cooled down successfully to the operation temperature from room temperature under gravity-assistance. When the vapor-liquid interface was present in the liquid core of the primary evaporator, temperature oscillation was observed under low power levels. The heat transfer capability of the CLHP increased as the height between the liquid and vapor lines increased. For instance the heat transfer capability of the CLHP was 8, 11 and 16 W respectively when the liquid line was 0, 3.4 and 6.4 cm below the vapor line. The gas reservoir volume, effective pore diameter of the primary evaporator wick and working fluids were identified as the three key parameters affecting the heat transfer capability of the CLHP. The heat transfer capability of the CLHP with oxygen as the working fluid was almost twice of that with nitrogen as the working fluid.

3.3 Type C

3.3.1 System structure

Fig.7 shows the schematic of this type of CLHP. Compared with an ALHP, the CLHP has an additional secondary evaporator, secondary CC and secondary condenser in addition to the gas reservoir. The secondary evaporator and CC are attached directly to the cryogenic heat sink and is connected in series with the primary and secondary condenser lines. The structure of the secondary evaporator and CC is generally the same as that of the primary evaporator and CC.

3.3.2 Supercritical startup

For the CLHP with type C to realize the supercritical startup, the secondary evaporator method is generally used and the supercritical startup process is similar to that of type B. However for type C, the vapor generated in the secondary evaporator can establish one-way circulation in the loop, and continuous application of heat load to the secondary evaporator can be adopted.

3.3.3 Experimental results

Within this category, Khrustalev et al.[26-28] experimentally investigated an oxygen-charged CLHP as flexible thermal links for cryocoolers. The outer diameter and length of the evaporator were 20 and 20mm respectively, and the transport distance was about 600mm. In the experiment, the primary and secondary condensers were cooled by a cryocooler, and the CLHP was placed in a vacuum chamber with temperature-controlled shrouds. The results showed that the CLHP can reliably and predictably achieve the supercritical startup and operate with the heat load range at the primary evaporator from 0.5W to 9W with zero power on the secondary evaporator. The evaporator temperature was maintained at 75K and 100 K respectively when the shroud temperature of was approximately 170K and 290K The CLHP could transport 9W when the primary evaporator was 5 cm higher than the primary condenser.

3.4 Type D

3.4.1 System structure

Fig.8 shows a schematic view of this type of CLHP. Compared with an ALHP, the CLHP has an additional auxiliary loop composed of a secondary evaporator, secondary CC, secondary condenser and secondary loop line in addition to the gas reservoir. The structure of the secondary evaporator and CC is generally the same as that of the primary evaporator and CC.

3.4.2 Supercritical startup

For the CLHP with type D to realize the supercritical startup, the auxiliary loop method is used to

provide cooling and liquid saturation of the primary evaporator wick of the CLHP. As the cryogenic heat sink takes effect, the temperature of the secondary evaporator and secondary CC begins to drop quickly, as well as the primary and secondary condensers. As the secondary evaporator wick is saturated with liquid, heat load is applied to start up the auxiliary loop. The vapor generated in the secondary evaporator push the condensate in the primary condenser into the primary evaporator and CC through the primary liquid line. Starting heat load is applied on the primary evaporator when its wick is fully saturated with liquid.

3.4.3 Experimental results

Type D CLHP has considerable potentials for spacecraft thermal control, and many experimental investigations were conducted, which are summarized in Table 1 and briefly reviewed below. .

Yun et al.[29] developed a CLHP and conducted the tests in a thermal-vacuum chamber for passive optical bench cooling applications. Ethane was selected as the working fluid to provide an operating temperature range of 215-218K. The outer diameter and length of the evaporator were 16 and 150mm, respectively. All the transport lines were arranged in a serpentine style and plated with gold to minimize parasitic heat losses. The experimental results clearly demonstrated the capability of type D CLHP, i.e. it could start up reliably from a supercritical temperature of 335K to achieve a normal operating temperature of 215K by using the secondary evaporator. With 5W applied to the secondary evaporator, the CLHP achieved a 50W heat transport capability at 215K. A power cycle test was performed showing that the system could adapt to rapid power changes. In addition, a heater located in the liquid line was required to shut down the system in order to prevent the rapid decrease of the instrument temperature during the safe mode, because simply turning power off to the primary and secondary evaporators cannot shut down the system.

Hoang et al.[30-34] first designed, fabricated and performance tested a proof-of-concept CLHP with nitrogen and hydrogen as the working fluids in the initial research phase. Test results indicated that the CLHP was capable of realizing supercritical startup and operating reliably, and the heat transport capability could reach 50W×m (i.e. 20W over a distance of 2.5m) and 12.5W×m (i.e. 5W over a distance of 2.5m) for nitrogen and hydrogen as the working fluids respectively with 1/8" OD vapor line and 3/32" OD liquid line. In the following, hydrogen-charged and across-gimbal nitrogen-charged CLHPs with weight/volume design optimization were developed and experimentally investigated. The optimized hydrogen-charged CLHP was able to start up from an initially supercritical condition and operate in a very "hot" environment of 235K. The cryocooling transport limit was 25W×m in 80K shroud and 22.5W×m in 235K. Throughout the test, it demonstrated a robust/reliable operation and resilience in all aspects of operation such as severe power cycling, low power long-duration runs, and it did not fail unexpectedly or exhibit noticeable anomalies. The optimized across-gimbal nitrogen-charged CLHP was experimentally investigated by both the mechanical demonstration unit and thermal demonstration unit, and Fig.9 shows the detailed structure of the across-gimbal nitrogen-charged CLHP. In the mechanical demonstration unit, the motor controller and peripheral electronics were programmed to autonomously rotate both azimuth and elevation coils in a prescribed manner. A strange phenomenon was found that the 1/16"OD lines (being more flexible) lasted even shorter than the 3/32" OD line perhaps due to a stress concentration on the 1/16"OD lines. In the thermal demonstration unit, the experimental results show that the CLHP can realize the supercritical startup successfully in less than 90 minutes with 5W applied to the secondary evaporator and 298K surrounding; the heat transport capacity can reach 5W over a transport distance of 4.3meters; the CLHP can operate with a small heat load applied to the primary evaporator for a long duration as long as the parasitic heat load is managed; the CLHP exhibits good power cycling characteristics, and it responds extremely

well with the changes of heat loads applied to the primary evaporator.

Bugby et al.[35, 36] developed three CLHPs for solving important problems in cryogenic integration. The three devices are an across-gimbal CLHP, a short transport length miniaturized CLHP and a long transport length miniaturized CLHP. The across-gimbal CLHP was designed with nitrogen as the working fluid with a heat transport range of 2-20W, and the coils should sustain at least 500 thousand cycles. Both the short and long transport length CLHPs utilized neon as the working fluid and operated at the temperature range of 30-40K, and Fig.10 shows the detailed structure of the short transport length neon-charged CLHP. Preliminary test results show that the short transport length CLHP is able to transport a heat load of 0.1-2.5W applied to the primary evaporator. The "ON" and "OFF" conductance is about 1 and 1400W/K respectively. While the long transport length CLHP is able to transport a heat load of 0.1-0.8 W applied to the primary evaporator. The "ON" conductance is about 0.7 W/K, and the "OFF" resistance is estimated to be over 5000 K/W.

Gully et al.[37] developed a nitrogen-charged CLHP, and the general design, the instrumentation and the experimental results of the thermal response of the CLHP were presented, analyzed and discussed both in the transient phase of cooling from room temperature (i) and in stationary conditions (ii). During phase (i), even in a severe radiation environment, the secondary loop helped to condense the fluid and was very efficient to chill the primary evaporator. During phase (ii), the effects of transferred power, filling pressure and radiation heat load for two basic configurations of cold reservoir of the secondary loop were studied. A maximum heat load of 19W with a corresponding limited temperature difference of 5K was achieved across a 0.5m distance. A small heating power (0.1W) applied to the shunted cold reservoir allowed to maintain a constant subcooling (1K). The CLHP behaved as a capillary pumped loop (CPL) in such a configuration, with the cold reservoir being the compensation chamber of the thermal link. The radiation

heat loads may affect significantly the thermal response of the system due to boiling process of liquid and large mass transfer towards the gas reservoir.

Zhao et al.[38, 39] designed and experimentally investigated a nitrogen-charged CLHP with parallel condenser structure. Experimental results confirmed that the CLHP could operate reliably with a high heat transport capacity up to 41W and a limited temperature difference of 6K across a 0.48m transport distance, and the supercritical startup and power cycling characteristics were also investigated. The possible fluid inventory range of the CLHP was calculated based on the analysis of phase distribution of vapor and liquid within the loop in a normal operation mode. Furthermore, a series of experiments were carried out with various filling pressures of the gaseous nitrogen at room temperature for validation of the fluid inventory range and identification of the optimal fluid inventory. The experimental results were compared with the calculation results, and the effect of different charged pressure on the performance of the CLHP was analyzed.

Bai et al.[40-43] developed a miniature nitrogen-charged CLHP as shown in Fig.11, and the principle and method to determine the charged pressure of the working fluid was presented in detail. The unique cylindrical condenser design could provide the interface with the cold finger of the cryocooler, and its operating characteristics were experimentally investigated. Based on the experimental results, important conclusions have been drawn: 1) with only 2.5W applied to the secondary evaporator, the CLHP can realize the supercritical startup, and the larger the heat load applied to the secondary evaporator, the sooner the temperature drop process of the primary evaporator; 2) when the heat load applied to the primary evaporator is no less than 3W, the primary evaporator can operate independently; whereas when it is smaller than 3W, the secondary evaporator must be kept in operation to assist the normal operation of the primary evaporator; 3) the CLHP has a heat transport capacity of 12W×0.56 m, and its thermal resistance

decreases with the increase of the heat load applied to the primary evaporator; 4) the CLHP has the ability to operate with a small heat load applied to the primary evaporator for a long time, and manifests good thermal control performance. In addition, the effects of component layout including the connection points of the gas reservoir to the working loop and the secondary loop line to the primary CC on the performance characteristics of the CLHP have been studied.

As a research focus and for comparison purpose, Table 1 presents a summary of the development and experimental results of CLHPs with type D including working fluids and operating temperature range, heat transport capacity, main size and some comments on the design and characteristics.

3.4.4 Modeling development

So far, quite a few modeling and theoretical studies have been carried out on ALHPs including the steady-state and transient performance as well as the startup characteristics [44-57]. Compared with ALHPs, the modeling and theoretical investigation on the operating characteristics of CLHPs is quite limited and obviously inadequate, and further study is still needed.

In Ref.[58], a steady-state mathematical model of a nitrogen-charged CLHP was established based on the conservations of mass, momentum and energy of each component, and the modeling results including the heat transport capacity and operating temperature variation trend showed good agreement with the experimental data. Based on the mathematical model, parametric analysis including the effects of heat sink temperature, parasitic heat load from the ambient, adverse elevation and heat load applied to the secondary evaporator on the operating temperature of the CLHP was conducted, and several important conclusions have been drawn. In Ref.[59], the mathematical model of the supercritical startup of a nitrogen-charged CLHP was established based on the nodal network method, and the supercritical startup process was divided into three stages according to the function and feature of the evaporator wicks: stage 1 is the

cooling of the secondary evaporator; stage 2 is the cooling of the primary evaporator and stage 3 is the startup of the main loop. Note that, the cooling of the secondary evaporator is the prerequisite to startup the auxiliary loop, and the startup of the auxiliary loop can realize the cooling and liquid saturation of the primary evaporator, which is the prerequisite to startup the main loop. Key factors affecting the supercritical startup performance was analyzed, and conclusions below have been drawn: a higher working fluid charged pressure and an enhanced thermal conductance between the secondary CC and heat sink can both shorten the time needed to complete the cooling of the secondary evaporator; a smaller parasitic heat load from the ambient and a larger heat load applied to the secondary evaporator can both shorten the time needed to complete the cooling of the primary evaporator; when the parasitic heat load is relatively large, it is possible that the primary evaporator wick can never be saturated with liquid, and the supercritical startup of CLHPs will fail; a larger parasitic heat load from the ambient can result in a higher steady-state operating temperature of the primary evaporator; a larger startup heat load can shorten the time needed to complete the startup of the main loop.

3.4.5 Design optimization

In order to put CLHPs into space applications, it is necessary to reduce its weight/volume considerably enhance its heat transport capacity and manage the parasitic heat load effectively, and design optimization plays an important role to reach such a goal.

Generally, the gas reservoir is disproportionally larger than any other component of the CLHP, i.e. its volume is several tens times larger than the working loop volume, so any weight/volume reduction scheme must focus on the gas reservoir. As the gas reservoir volume is proportional to the amount of liquid in the system needed for normal operation, an obvious solution to the weight/volume problem is to minimize the loop liquid volume. Another not-so-obvious way to reduce the system pressure during the supercritical

startup even without a gas reservoir is to condense as much liquid as required to realize the startup of the secondary evaporator. Based on the two schemes mentioned above, Hoang et al.[60] conducted an optimization design on a hydrogen-charged CLHP by the miniaturization of loop components especially the liquid-filled components such as the primary and secondary evaporators, condensers and liquid transport lines and incorporation of a swing volume at the inlet of the primary condenser. Results of analyses indicated that a 10-fold decrease of the gas reservoir volume was possible providing that high performance wicks with pore size of <1.5micron were employed in both the primary and secondary evaporators.

To enhance the heat transport capacity, Zhao et al.[38] designed and experimentally investigated a nitrogen-charged CLHP with improved condenser structure. The improved condenser of the CLHP was made of a cubic copper block with machined parallel pipes inside. The flow resistance of the working fluid in this improved condenser structure is reduced considerably. Furthermore, the heat transfer performance between the condenser and the heat sink could be improved effectively compared with conventional condenser design by the elimination of additional thermal contact resistance. Experimental results confirmed that the heat transport capacity of the CLHP could be enhanced up to 41W across a 0.48m transport distance.

To manage the parasitic heat load from the ambient, several designs have been proposed including the employment of transport lines with gold-plated exterior surface and miniaturized OD and the coaxial design of the primary liquid line and the secondary loop line. The employment of transport lines with gold-plated exterior surface and miniaturized OD can effectively reduce the parasitic heat load by decreasing the heat transfer area and absorption rate of the transport lines simultaneously. For the coaxial design, the primary liquid line is coaxially within the secondary loop line, and the parasitic heat load on the primary liquid line can be inhibited considerably without introducing other components, which is a very

good choice.

3.5 Type E

3.5.1 System structure

To enable cryocooling of a heat source with a large area, the CLHP with type E has been developed, and Fig.12 shows the schematic of this type of CLHP. As shown in Fig.9, the CLHP is composed of an evaporator, a condenser, a capillary pump, a CC and transport lines plus a gas reservoir. The capillary pump and CC are attached directly to the heat sink. A notable change in this design is that the capillary pump is utilized not to acquire heat directly from the heat sources but simply to generate fluid flow in the loop. An electrical heater, bonded to the capillary pump body, provides necessary heat input for operation. Meanwhile, the evaporator is just composed of flexible small-diameter smooth-walled pipelines with no wicks inside, which has very good adaptability to heat sources with large area and complex structure.

3.5.2 Supercritical startup

For the CLHP with type E to realize the supercritical startup, the capillary pump method has been proposed. The capillary pump method is to utilize the capillary pump as an assistant to realize the cooling and liquid accumulation of the evaporator of the CLHP. For a CLHP adopting the capillary pump method, the supercritical startup process is as follows: prior to startup, the whole CLHP is initially at the ambient state; as the cryogenic heat sink takes effect, the temperature of the capillary pump and CC begins to drop quickly as well as the condenser, and fluid condensation will occur when it drops to the saturation temperature with respect to local pressure; with continuous condensation of working fluid in the CC, the capillary pump wick will be fully saturated with liquid, under this situation, heat load from an electrical heater can be applied to the capillary pump to make it start; once the capillary pump is started, the vapor generated in the capillary pump can push the condensate in the condenser into the evaporator through the

transport lines, which could realize the temperature drop and subsequent liquid accumulation in the evaporator; with continuous liquid accumulation in the evaporator, heat load from the heat source can be applied to the evaporator to complete the supercritical startup of the CLHP.

3.5.3 Experimental results

Hoang et al. [61, 62] designed and experimentally investigated CLHPs with neon and helium as the working fluids respectively. Fig.13 shows the test unit of the Ne-CLHP, where the outer diameter and length of the capillary pump wick were 5.3 and 50.8mm respectively. In the Ne-CLHP experiments, the pump heater was activated with 1W to start fluid circulation in the loop. It cooled down the evaporator plate effortlessly from a supercritical condition (100K) with a rate of 30-40K per hour, and no special wick priming procedure was required. The maximum cooling capacity was 4.2W over an evaporator area of $48in^2$ with 2.5W applied to the capillary pump. Temperature control of the evaporator under loads was easily accomplished by simply regulating the power input to the capillary pump. Increasing the capillary pump heater power lowered the evaporator temperature, and conversely, decreasing the pump heater power raised the evaporator temperature. Low power operation was also demonstrated with 1W on the evaporator and 0.5W on the capillary pump. Effects of fluid charge level on the Ne-CLHP operation were also investigated: overcharging the test loop would result in partial liquid blockage of both reservoir and condenser, making the heat transfer between the condenser and cryocooler less effective. In order to dissipate the same amount of heat, the condenser-to-cryocooler temperature difference had to increase. With the exception of higher saturation temperatures for overcharging, no other performance difference was detected including the capillary pump power limit and the evaporator cooling capacity.

He-CLHP was the first-ever operational capillary cryocooling transport in the 3-5K temperature range. The narrow two-phase range of Helium (2.2-5.1K), sizing the components and charging the loop had to be

extremely accurate. In the He-CLHP experiments, a Helium dewar was employed to act as the heat sink at ~2.5-2.7K. In the supercritical startup, when the loop temperatures dropped below 2.7K, 10mW was applied to the capillary pump to start the fluid circulation in the loop, about 8mins later, 15mW was applied to the evaporator to begin the operation, and the He-CLHP finally reached steady state with the saturation temperature leveling off just below 2.8K. The power cycling characteristics of the He-CLHP was investigated. With the pump power kept at 50mW, the evaporator power was stepped up to 60mW from 50mW, the loop temperatures changed very little, but the evaporator temperature increased by 0.25K. The evaporator power was subsequently stepped up with a 10mW increment until it reached the anticipated limit of 100mW. Again the loop temperatures changed little (went up from 3.5K to 3.7K) but the evaporator temperature went up ~0.7K for every 10mW power step-up. In another test, the evaporator was kept at 50mW while the pump power was reduced slowly from 35mW. As the pump power decreased, the evaporator temperature increased as expected. When it got to 25mW, the evaporator temperature was able to level off at 5K.

4 Comparative analyses

4.1 System structure

Generally, a gas reservoir with a relatively large volume is an indispensable component of all types of CLHPs. This is due to the fact that a CLHP operate at very low temperature range, the working fluid in the loop is in the two-phase state and its pressure seldom exceeds several atmospheres when it is in operation. However when it is idle and the whole system is at ambient temperature, far higher than the critical temperature of the cryogenic working fluid. The working fluid is in the supercritical state. As the specific volume of supercritical gas is generally over two orders in magnitude larger than that of saturated

liquid of the cryogenic working fluid under the same pressure, the pressure in the loop would reach several hundred atmospheres or even higher. Without the employment of a gas reservoir, a much higher demand of structural robustness and sealing is required for CLHPs as well as the storage security. The idle pressure of the CLHP can be reduced considerably by employing a gas reservoir with a relatively large volume. The reduction of idle pressure also mitigated the difficulties of startup of a CLHP, as discussed in detail below. In addition to the gas reservoir, additional components are required to assist the smooth startup and operation of a CLHP, as summarized in Table 2 From the structure consideration, Type A CLHP is based on the gravity assisted method, and has the simplest structure; while the CLHP with type D adopting the auxiliary loop method has the most complex structure. It is of note that the CLHPs with types A-D are suitable to concentrated heat sources but type E is only applicable to heat sources with large areas.

4.2 Supercritical startup

The startup capability is one of the key aspects to evaluate the LHP performance, and is also the first issue to be resolved to for any practical applications. For an ALHP, the working fluid inside is in the two-phase state at the ambient state, and the evaporator wick can be always saturated with liquid through proper of the CC volume and working fluid inventory. Under such a situation, heat load can be directly applied to the evaporator to start up the ALHP. However, the startup process of a CLHP is more complicated than that of an ALHP as the fluid is at the supercritical state . The evaporator wick must be cooled down and saturated with liquid prior to the application of a heat load.

In order to realize the supercritical startup, several methods have been proposed including the gravity assisted method, the secondary evaporator method, the auxiliary loop method and the capillary pump method, as detailed in section 3. Table 3 presents the comparison of supercritical startup for CLHPs with

different types. As shown in Table 3, the gravity-assisted method is proven to be very effective in achieving the supercritical startup without additional power consumption. However as it depends on the gravity as an assistant, it is not suitable for space applications. Type B and C CLHPs both adopt the secondary evaporator method but with different structures. Type B is difficult to establish one way circulation of the working fluid in the loop due to its location. The length and diameter of the vapor and liquid transport lines should be designed properly to minimize the flow resistance in order to provide effective cooling and liquid saturation of the primary evaporator wick. It is expected that the transport distance of the CLHP is short. . However for type C, one way circulation of working fluid in the loop can be effectively established, which provided better cooling and liquid saturation of the primary evaporator wick. The auxiliary loop method and the capillary pump method are both very effective to help realize the supercritical startup of CLHPs, but with added complexities in the loop.

4.3 Heat transport capacity

The heat transport capacity of a CLHP is decided not only by the fluid properties but also the system structure. Section 2 shows that cryogenic fluids possess much lower Dunbar Parameter, implying a smaller heat transport capacity than that of ALHPs. The additional components of a CLHP and their arrangement to assist smooth startup would bring additional flow resistance that affect its heat transport capability. Type A CLHP has good heat transfer capability due to the gravity assistance measure and no additional components added in the main loop. For type B, although a secondary evaporator is added in series inside the condenser, the simple design of the secondary evaporator (i.e. a pipe with axial grooves machined on its inner surface) would not cause large flow resistance. The introduce of the secondary evaporator would not affect the heat transport capacity of the CLHP significantly . For type C, the working fluid has to pass through the fine porous wick of the secondary evaporator in the circulation, which

increased the flow resistance , resulting in a decreased heat transport capacity. For type D, when the secondary evaporator is not in operation, it does not bring additional flow resistance as the auxiliary loop is in parallel with the main loop , and the heat transport capacity is not affected. When the secondary evaporator is in operation, however, it will lead to an increased mass flowrate in the primary condenser and primary liquid line. The increased pressure drop would reduce the heat transport capacity of the CLHP Type E has a fixed distance between the heat source and heat sink, the working fluid has to travel back and forth between the heat source and heat sink several times. The increase in the total travel distance of the working fluid increase the total pressure drop of working fluid circulating along the loop and would decrease the heat transport capacity of the CLHP considerably.

4.4 Effect of parasitic heat load

The parasitic heat load is the heat absorbed from the ambient by LHPs when the temperatures of the entire LHP or some components are lower than the ambient temperature. For an ALHP, the parasitic heat needs to be considered when the operating temperature is lower than the ambient temperature or the heat sink temperature is lower than the ambient temperature. When the heat load applied to the evaporator is small, the intake of the parasitic heat load would increase the operation temperature significantly. and decrease the system conductance. The existence of the variable conductance mode in ALHPs operation is mainly due to the parasite heat. The problem of parasite heat is mitigated at higher heat loads. The increased mass flowrate of the working fluid in the loop would inhibit the effect of parasitic heat load. Generally speaking, the parasitic heat load is not a big issue during the normal operation of an ALHP as the temperature difference between the LHP components and the ambient is usually very small. . In some cases such as in the spacecraft thermal control, the parasitic heat load can be utilized to control the

operating temperature of ALHPs within the required range when the heat load applied to the evaporator is subjected to a large range of variation. Most of the parasite heat can be managed effectively through proper insulation..

Different from the ALHP, the issue of parasitic heat load for CLHP becomes severe, and it may even stop its normal operation . That is due to two main reasons: i) the temperature difference between the CLHP components and the ambient is rather large, which would produce high parasite heat, and ii) the heat transport capability is much smaller for a CLHP, and the negative effect of parasitic heat load on the CLHPs operation becomes more obvious especially for the antigravity operation. Under an anti-gravity operation, the temperature of the return liquid would rise continually as it flows along the liquid transport line due to the parasite heat intake and at the same time, its pressure drops constantly due to the gravity effect. The return liquid may reach a saturated state and begin to boil. In a more server case, the temperature of the return liquid may exceed its critical temperature and become supercritical at the outlet of the liquid transport line. Under these situations , the CLHP cannot operate normally due to the failure in liquid replenishment to the evaporator wick.

To ensure successful supercritical startup and normal operation of CLHPs, strict insulation measures must be employed to reduce the parasitic heat load In most ground experiments, CLHPs are generally placed in a thermal-vacuum chamber, and all the CLHP components except the gas reservoir are protected by multi-layer insulation materials. In some situations, a low temperature shield between the CLHP and the inner wall of the thermal-vacuum chamber may be utilized, which effectively create a cold environment for CLHPs and minimize the adverse effect of parasitic heat load.

It is of note that Type D CLHP has the ability to manage the problem of parasitic heat load, especially when the heat load applied to the primary evaporator is very small. That is because the auxiliary

loop is in parallel with the main loop. When the primary evaporator is in normal operation, the secondary evaporator can be kept in operation simultaneously, which can increase the mass flowrate of the working fluid and inhibit the temperature rise due to parasite heat. The increase in the subcooling of the returning liquid is crucial for the stable operation of the primary evaporator for Type D CLHP, especially under low heat loads. .

4.5 Design optimization

There are still many scope to improve the performance of LHPs. For ALHPs, most recent studies focus on the performance improvement of the evaporator wick, and quite a few researchers have developed and investigated the biporous or bidisperse wicks to enable the evaporator with high capillary pumping capability, and low flow resistance yet with excellent evaporative heat transfer performance[63-67]. Clearly similar or improved wick structure could be applied to CLHPs. In addition, an optimized consideration of the weight/volume reduction, enhancement in heat transport capacity and management of the parasitic heat load is essential to achieve better performance. Some of these requirements may be contradictory sometimes. For instance the employment of small diameter transport lines can reduce the system weight/volume and the parasitic heat load from the ambient, but it also decrease the heat transport capacity of the CLHP. Clearly much progress has been made on the design optimization of CLHPs, further comprehensive and in-depth research is still needed to progress the application of CLHPs into space in the near future.

5 Conclusions

In this paper, the development of CLHPs has been comprehensively reviewed, where the CLHPs are

categorized into five types mainly based on the system structural characteristics. A comparative study both between CLHPs and ALHPs and among different types of CLHPs has been conducted covering a variety of aspects including the working fluid, system structure, supercritical startup, heat transport capacity, effect of parasitic heat load as well as the design optimization, in order to clarify the principal differences in the performance characteristics and application fields for CLHPs with different types. This work contributes to a better understanding of the development and operating principle and characteristics of CLHPs, and can guide the design and application of these devices.

ACKNOWLEDGEMENTS

This work was supported by Beijing Natural Science Foundation (No. 3144031), the National Natural Science Foundation of China (No. 51306009) and the EU Marie Curie Actions-International Incoming Fellowships (FP7-PEOPLE-2013-IIF-626576).

References

[1] Y.F. Maydanik, Loop heat pipes, Applied Thermal Engineering 25(2005) 635-657

[2] J. Ku, Operating characteristics of loop heat pipes, SAE paper, No.1999-01-2007,1999

[3] G.H. Wang, D. Mishkinis, D. Nikanpour, Capillary heat loop technology: space applications and recent Canadian activities, Applied Thermal Engineering 28(2008) 284-303

[4] F. Bodendieck, B. Hollenbach, K. Goncharov, Propylene LHP for the AMS Cryo-Cooler Thermal Control System, AMS 02 Technical Note, Document No. AMS-OHB-TEN-003, 2005

[5] V. Perotto, S. Tavera, K. Goncharov, Development of improved 1500W Deployable Radiator with Loop Heat Pipe, SAE paper, No.2000-01-2458, 2000

[6] M.L. Parker, Modeling of loop heat pipe with applications to spacecraft thermal control, Pennsylvania: Faculty of Mechanical Engineering and Applied Mechanics, University of Pennsylvania , 2000

[7] Eric W. Grob, Mission performance of the GLAS thermal control system-7 years in orbit, AIAA Paper, No.2010-6029, 2010

[8] Jose I. Rodriguez, Arthur Na-Nakornpanom, In-flight performance of the test loop heat pipe heat rejection system-seven years in space, AIAA Paper, No. 2012-3500, 2012

[9] N. Wang, Z. Cui, J. Burger, et al., Transient behaviors of loop heat pipes for alpha magnetic spectrometer cryocoolers, Applied Thermal Engineering 68 (2014) 1-9

[10] J. Xu, X. Ji, W. Yang, et al., Modulated porous wick evaporator for loop heat pipes: Experiment, International Journal of Heat and Mass Transfer 72 (2014) 163-176

[11] J. Li, D. Wang, G.P. Peterson, Experimental Studies on a High Performance Compact Loop Heat Pipe with Flat Square Evaporator for High Power Chip Cooling, Applied Thermal Engineering 30(2010) 741-752

[12] M. Mitomi, H. Nagano, Long-distance loop heat pipe for effective utilization of energy, International Journal of Heat and Mass Transfer 77 (2014) 777-784

[13] A.L. Phillips, K.L. Wert, Loop Heat Pipe Anti Icing System Development Program Summary, SAE Paper, No. 2000-01-2493, 2000

[14] L. Bai, G. Lin, D. Wen, et al. Experimental investigation of startup behaviors of a dual compensation chamber loop heat pipe with insufficient fluid inventory, Applied Thermal Engineering 29 (2009) 1447-1456

[15] J. Feng, G. Lin, L. Bai, Experimental investigation on operating instability of a dual compensation chamber loop heat pipe, Science in China Series E: Technological Sciences 52(2009) 2316-2322

[16] G. Lin, N. Li, L. Bai, et al. Experimental investigation of a dual compensation chamber loop heat pipe, International Journal of Heat and Mass Transfer 53(2010) 3231-3240

[17] Y.F. Maydanik, S. Vershinin, M. Chernysheva, et al. Investigation of a compact copper-water loop heap pipe with a flat evaporator, Applied Thermal Engineering 31(2011) 3533-3541

[18] V.G. Pastukhov, Y.F. Maydanik, C.V. Vershinin, et al. Miniature Loop Heat Pipes for electronics cooling, Applied Thermal Engineering 23(2003) 1125-1135

[19] Y.F. Maydanik, V.V. Sergey, G. Pastukhov, et al., Loop Heat Pipes for Cooling Systems of Servers, IEEE TRANSACTIONS ON COMPONENTS AND PACKAGING TECHNOLOGIES 33(2)(2010) 416-423

[20] V.G. Pastukhov, Y.F. Maydanik, Low-noise cooling system for PC on the base of Loop Heat Pipes, Applied Thermal Engineering 27(2007) 894-901

[21] Y.F. Maydanik, M.A. Chernysheva, V.G. Pastukhov, Review: Loop heat pipes with flat evaporators, Applied Thermal Engineering 67 (2014) 294-307

[22] H. Pereira, F. Haug, P. Silva, et al., Cryogenic loop heat pipes for the cooling of small particle detectors at CERN, Advances in Cryogenic Engineering: Transactions of the Cryogenic Engineering Conference 55(2010) 1039-1046

[23] Q. Mo, J. Liang, A novel design and experimental study of a cryogenic loop heat pipe with high heat transfer capability, International Journal of Heat and Mass Transfer 49(2006) 770-776

[24] Q. Mo, J. Liang, J. Cai, Investigation of the effects of three key parameters on the heat transfer capability of a CLHP, Cryogenics 47(2007) 262-266

[25] Q. Mo, J. Liang, Operational performance of a cryogenic loop heat pipe with insufficient working fluid inventory, International Journal of Refrigeration 29(2006) 519-527

[26] D. Khrustalev, S. Semenov, Advances in Low-Temperature, Cryogenic, and Miniature Loop Heat Pipes, Presentation at the 12thAnnual Spacecraft Thermal Control Technology Workshop, El Segundo, March 2003

[27] D. Khrustalev, Cryogenic Loop Heat Pipes as Flexible Thermal Links for Cryocoolers, Proc. of the 12th Int. Cryocooler Conference, June 18-20, 2002, Cambridge, MA, USA, 709-716

[28] D. Khrustalev, Test Data for a Cryogenic Loop Heat Pipe Operating in the Temperature Range from 65k to 140K, Presentation at the International Two-Phase Thermal Control Technology Workshop, Mitcheville, MD, September 24-26, 2002

[29] J. Yun，E. Kroliczek，L. Crawford, Development of a Cryogenic Loop Heat Pipe (CLHP) for Passive Optical Bench Cooling Applications, SAE paper, No. 2002-01-2507

[30] T.T. Hoang, T.A. O'Connell, D.K. Khrustalev, Development of a Flexible Advanced Loop Heat Pipe for Across-Gimbal Cryocooling, Proceedings of SPIE Vol. 5172 (2003) 68-76

[31] T.T. Hoang, T.A. O'Connell, D.K. Khrustalev, et al., Cryogenic Advanced Loop Heat Pipe in

Temperature Range of 20-30K, 12th International Heat Pipe Conference, Moscow, 2002

[32] T.T. Hoang, T.A. O'Connell, J. Ku, Management of Parasitics in Cryogenic Advanced Loop Heat Pipes, AIAA paper, No.2003-0346, 2003

[33] T.T. Hoang, T.A. O'Connell, Performance demonstration of flexible advanced loop heat pipe for across-gimbal cryocooling, AIAA paper, No. 2005-5590, 2005

[34] T.T. Hoang, T.A. O'Connell, J. Ku, et al., Performance Demonstration of a Hydrogen Advanced Loop Heat Pipe for 20-30K Cryocooling of Far Infrared Sensors, Proceedings of SPIE, Vol.5904, 2005

[35] D. Bugby, B. Marland, C. Stouffer, et al., Across-gimbal and miniaturized cryogenic loop heat pipes, Space technology and applications international forum-STAIF (2003) 218-226

[36] D. Bugby, B. Marland, C. Stouffer, et al., Development of advanced tools for cryogenic integration, Advances in Cryogenic Engineering: Transactions of the Cryogenic Engineering Conference 49(2004) 1914-1922

[37] P. Gully, Q. Mo, T. Yan, et al., Thermal behavior of a cryogenic loop heat pipe for space application, Cryogenics 51 (2011) 420-428

[38] Y. Zhao, T. Yan, J. Liang, Experimental study on a cryogenic loop heat pipe with high heat capacity, International Journal of Heat and Mass Transfer 54(2011) 3304-3308

[39] T. Yan, Y. Zhao, J. Liang, et al., Investigation on optimal working fluid inventory of a cryogenic loop heat pipe, International Journal of Heat and Mass Transfer 66 (2013) 334-337

[40] L. Bai, G. Lin, H. Zhang, et al. Experimental study of a nitrogen-charged cryogenic loop heat pipe, Cryogenics, 52 (2012) 557-563

[41] L. Bai, G. Lin, H. Zhang, et al. Operating characteristics of a miniature cryogenic loop heat pipe, International Journal of Heat and Mass Transfer, 55 (2012) 8093-8099

[42] L. Bai, G. Lin, H. Zhang, et al. Effect of component layout on the operation of a miniature cryogenic loop heat pipe, International Journal of Heat and Mass Transfer, 60 (2013) 61-68

[43] C. Du, L. Bai, G. Lin, et al., Determination of charged pressure of working fluid and its effect on the operation of a miniature CLHP, International Journal of Heat and Mass Transfer 63(2013) 454-462

[44] M.A. Chernysheva, S.V. Vershinin, Y.F. Maydanik, Operating temperature and distribution of a working fluid in LHP, International Journal of Heat and Mass Transfer 50 (2007) 2704-2713

[45] L. Bai, G. Lin, H. Zhang, et al. Mathematical modeling of steady state operation of a loop heat pipe, Applied Thermal Engineering, 29 (2009), 2643-2654

[46] V.V. Vlassov, R.R. Riehl, Mathematical model of a loop heat pipe with cylindrical evaporator and integrated reservoir, Applied Thermal Engineering, 28(2008), 942-954

[47] T.T. Hoang, T.A. O'Connell, J. Ku, Mathematical modeling of loop heat pipes with multiple capillary pumps and multiple condensers, Part I – steady state simulations, AIAA paper, No.2004-5577, 2004

[48] T. Kaya, T.T. Hoang, J. Ku, Mathematical Modeling of Loop Heat Pipes, AIAA paper, No. 99-0477, 1999

[49] T.T. Hoang, T. Kaya, Mathematical Modeling of Loop Heat Pipes with Two-phase Pressure Drop, AIAA paper, No. 99-3448, 1999

[50] J. Ambrose, E. Buchan, B. Yendler, Modeling and Test Results for a Loop Heat Pipe with Parallel-Flow Condenser, AIAA paper, No. 2000-2280, 2000

[51] S. Launay, V. Sartre, J. Bonjour, Parametric analysis of loop heat pipe operation: a literature review, International Journal of Thermal Science, 46 (2007) 621-636

[52] L. Bai, G. Lin, D. Wen, Modeling and analysis of startup of a loop heat pipe, Applied Thermal Engineering 30 (2010) 2778-2787

[53] M.A. Chernysheva, V.G. Pastukhov, Y.F. Maydanik, Analysis of heat exchange in the compensation chamber of a loop heat pipe, Energy 55 (2013) 253-262

[54] B. Siedel, V. Sartre, F. Lefèvre, Numerical investigation of the thermohydraulic behaviour of a complete loop heat pipe, Applied Thermal Engineering 61 (2013) 541-553

[55] J. Li, G.P. Peterson, 3D heat transfer analysis in a loop heat pipe evaporator with a fully saturated wick, International Journal of Heat and Mass Transfer 54(2011) 564-574

[56] M.A. Chernysheva, Y.F. Maydanik, 3D model for heat and mass transfer simulation in flat evaporator of copper-water loop heat pipe, Applied Thermal Engineering 33-34(2012) 124-134

[57] M.A. Chernysheva, Y.F. Maydanik, Simulation of thermal processes in a flat evaporator of a copper-water loop heat pipe under uniform and concentrated heating, International Journal of Heat and Mass Transfer 55(2012) 7385-7397

[58] L. Bai, G. Lin, D. Wen, Parametric analysis of steady-state operation of a CLHP, Applied Thermal Engineering 30(2010) 850-858

[59] L. Bai, G. Lin, D. Wen, Modeling and analysis of supercritical startup of a cryogenic loop heat pipe, Journal of Heat Transfer-Transactions of ASME 133(2011) No.121501

[60] T.T. Hoang, T.A. O'Connell, J. Ku, et al., Design optimization of a hydrogen advanced loop heat pipe for space-based IR sensor and detector cryocooling, Proceedings of SPIE 5172(2003) 86-96

[61] T.T. Hoang, T.A. O' Connell, J. Ku, et al., Large Area Cryocooling for Far Infrared Telescopes, Proceedings of SPIE Vol. 5172 (2003) 77-85

[62] T.T. Hoang, T.A. O'Connell, D.A. Suhkov, Large Area Cooling with Cryogenic Loop Heat Pipes, AIAA paper, No. 2007-4272, 2007

[63] Z. Liu, H. Li, B. Chen, et al., Operational characteristics of flat type loop heat pipe with biporous wick, 58(2012) 180-185

[64] F. Lin, B. Liu, C. Huang, et al., Evaporative heat transfer model of a loop heat pipe with bidisperse wick structure, International Journal of Heat and Mass Transfer 54 (2011) 4621-4629

[65] F. Lin, B. Liu, C. Juan, et al., Effect of pore size distribution in bidisperse wick on heat transfer in a loop heat pipe, Heat Mass Transfer 47 (2011) 933-940

[66] R. Singh, A. Akbarzadeh, M. Mochizuki, Effect of Wick Characteristics on the Thermal Performance of the Miniature Loop Heat Pipe, Journal of Heat Transfer Vol. 131, paper No. 082601

[67] C. Yeh, C. Chen, Y.M. Chen, Heat transfer analysis of a loop heat pipe with biporous wicks, International Journal of Heat and Mass Transfer 52 (2009) 4426-4434

Table captions

Table 1 Summary of CLHPs with type D

Table 2 Added components for CLHPs with different types compared to ALHPs

Table 3 Comparison of supercritical startup for CLHPs with different types

Figure captions

Fig.1 Detailed structure of the evaporator and CC

Fig.2 Schematic of a typical LHP

Fig.3 Variation of Dunbar Parameter of ammonia and water

Fig.4 Variation of Dunbar Parameter of cryogenic working fluids

Fig.5 Schematic of the CLHP with type A

Fig.6 Schematic of the CLHP with type B

Fig.7 Schematic of the CLHP with type C

Fig.8 Schematic of the CLHP with type D

Fig.9 Detailed structure of across-gimbal N_2-CLHP[33]

Fig.10 Detailed structure of short transport length Ne-CLHP[35]

Fig.11 Detailed structure of N_2-CLHP with cylindrical condenser[41]

Fig.12 Schematic of the CLHP with type E

Fig.13 Detailed structure of the Ne-CLHP for large area cryocooling[62]

Table 1 Summary of CLHPs with type D

Authors (year)	No.	Working fluid and temperature range	Heat transport capacity	Main size	Comments
Yun et al. (2002)[29]	1	Ethane for 215-218K	50W on primary evaporator with 5W on secondary evaporator	Primary evaporator OD/Length: 16/150 mm Vapor line OD: 4.8mm Liquid line OD: 3.2mm	Supercritical startup, power cycling and recovery and shutdown were investigated
Hoang et al. (2003)[30-34]	1	Hydrogen for 20-30K Nitrogen for 80-110K	5W with a distance of 2.5m 20W with a distance of 2.5m	Primary evaporator OD/Length: 20/30 mm Vapor line OD/Length: 3.2/2540 mm Liquid line OD/Length: 2.4/2540 mm	Proof of Concept test with no optimization, supercritical startup capability and heat transport capacity were demonstrated
	2	Hydrogen for 20-30K	10W on primary evaporator with 2.5m transport distance	Primary evaporator OD/Length: 12/40 mm Vapor line OD/Length: 2.4/2500 mm Liquid line OD/Length: 1.6/2500 mm	Swing volume employed, Supercritical startup, power cycling, long duration low power and response to varying shroud temperature were investigated
	3	Nitrogen for 80-110K	5W on primary evaporator with 4.3m transport distance	Primary evaporator OD/Length: 12/40 mm Vapor line OD/Length: 2.4/2500 mm Liquid line OD/Length: 1.6/2500 mm	Across-gimbal design, swing volume employed, both mechanical and thermal demonstration units were tested
Bugby et al. (2004)[35-36]	1	Nitrogen for 80-100K	20W on primary evaporator	Primary evaporator OD/Length: 16/160 mm Vapor line OD: 3.2 mm Liquid line OD: 2.4 mm	Across-gimbal design, preliminary test conducted, operational idiosyncrasies in gravity field operation were found
	2	Neon for 30-40K	2.5W on primary evaporator with 0.15m transport distance	Primary evaporator Width/Length: 25/38mm Vapor line OD: 1.6 mm Liquid line OD: 0.8 mm	For short distance thermal link, and thermal switch performance was tested
	3	Neon for 30-40K	0.8W on primary evaporator with 2.5m transport distance	Primary evaporator Width/Length: 25/38mm Vapor line OD: 1.6 mm Liquid line OD: 1.1 mm	For long distance thermal link, and thermal switch performance was tested
Gully et al. (2011)[37]	1	Nitrogen for 80-120K	19W on primary evaporator with 0.5m transport distance	Primary evaporator OD/Length: 22/64 mm Vapor line OD/Length: 3/567 mm Liquid line OD/Length: 3/328 mm	Supercritical startup, effects of parasitic heat loads and employment of a thermal shunt were investigated
Zhao et al. (2011)[38-39]	1	Nitrogen for 80-120K	41W on primary evaporator with 0.48m transport distance	Primary evaporator OD/Length: 27/45 mm Vapor line OD/Length: 6/661 mm Liquid line OD/Length: 3/450 mm	Parallel condenser employed, and supercritical startup, power cycling and effect of charged pressure were investigated
Bai et al. (2012)[40-43]	1	Nitrogen for 80-110K	12W on primary evaporator with 0.56m transport distance	Primary evaporator OD/Length: 13/35 mm Vapor line OD/Length: 2/640 mm Liquid line OD/Length: 2/560 mm	Supercritical startup, heat load matching characteristics, power cycling and effects of charged pressure and component layout were investigated

Table 2 Added components for CLHPs with different types compared to ALHPs

Type	Added components	Structure complexity	Heat source
A	a gas reservoir	most simple	concentrated
B	a secondary evaporator and a gas reservoir	simple	concentrated
C	a secondary evaporator, a secondary CC, a secondary condenser and a gas reservoir	intermediate	concentrated
D	a secondary evaporator, a secondary CC, a secondary condenser, a secondary loop line and a gas reservoir	most complex	concentrated
E	an evaporator composed of flexible pipelines and a gas reservoir	intermediate	large area

Table 3 Comparison of supercritical startup for CLHPs with different types

Item	Type of CLHPs				
	A	B	C	D	E
Auxiliary method	gravity assisted method	secondary evaporator method	secondary evaporator method	auxiliary loop method	capillary pump method
Effectiveness	best	weak	good	good	good
Power consumption	no	yes	yes	yes	yes
Applicable field	ground	space and ground	space and ground	space and ground	space and ground

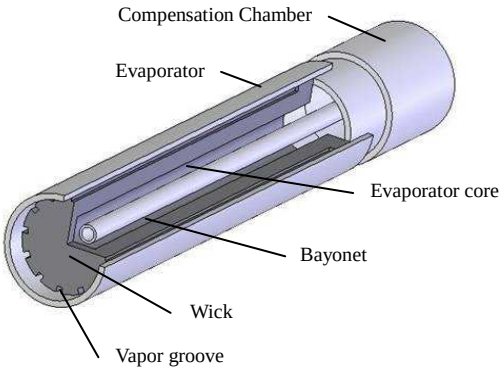

Fig.1 Detailed structure of the evaporator and CC

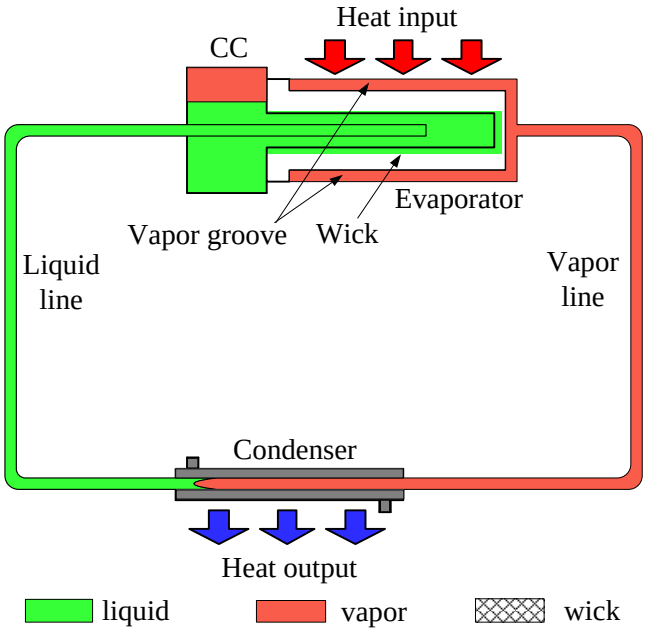

Fig.2 Schematic of a typical LHP

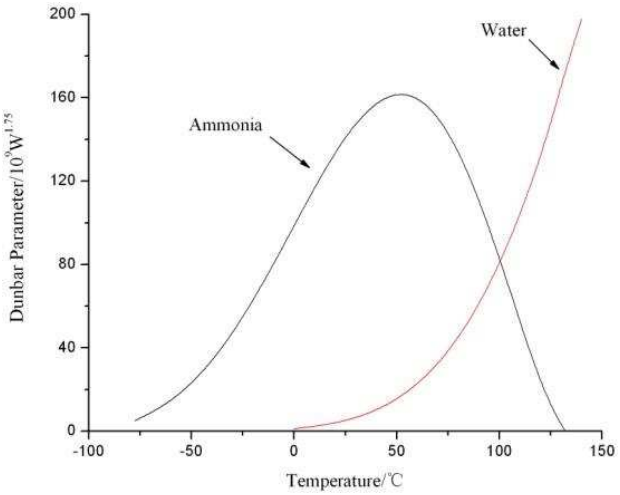

Fig.3 Variation of Dunbar Parameter of ammonia and water

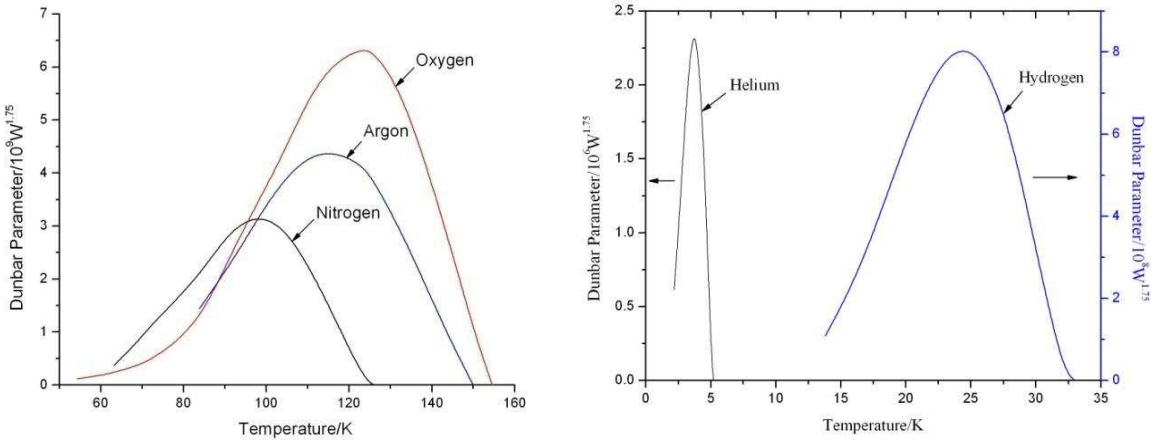

(a) Nitrogen, argon and oxygen (b) Hydrogen and helium

Fig.4 Variation of Dunbar Parameter of cryogenic working fluids

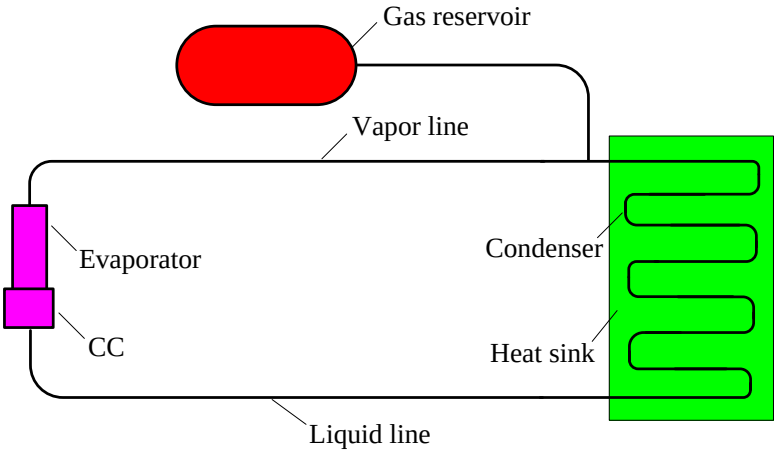

Fig.5 Schematic of the CLHP with type A

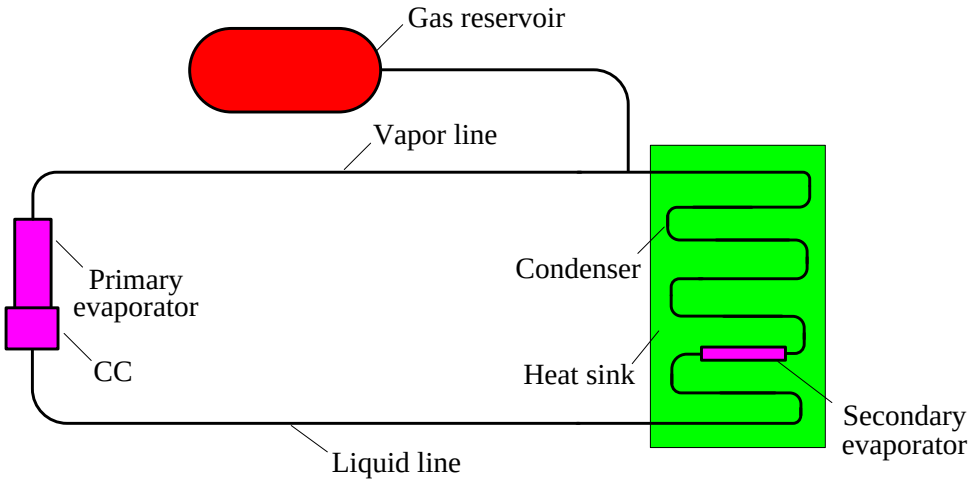

Fig.6 Schematic of the CLHP with type B

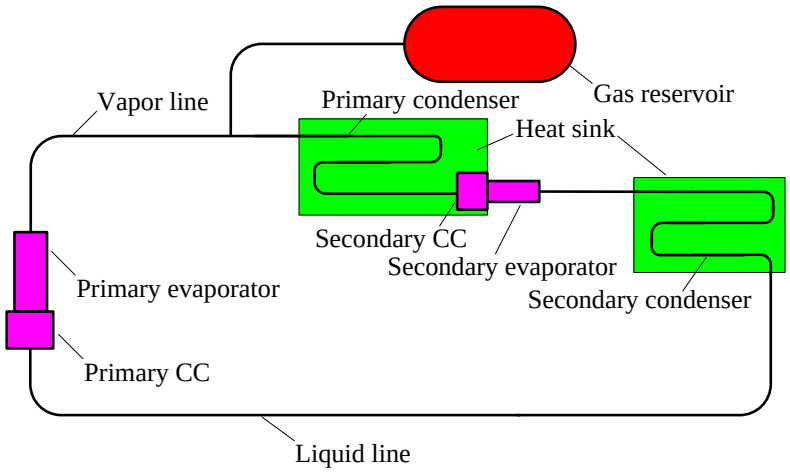

Fig.7 Schematic of the CLHP with type C

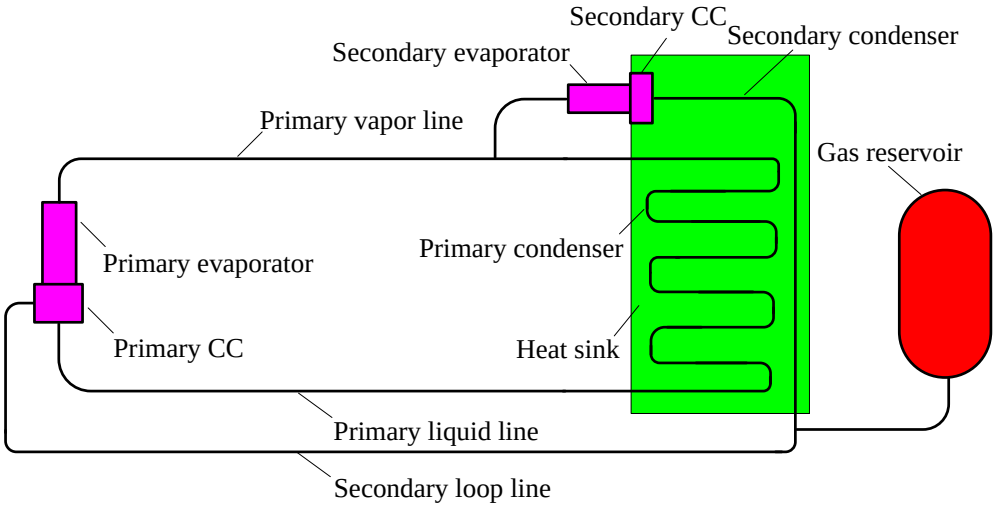

Fig.8 Schematic of the CLHP with type D

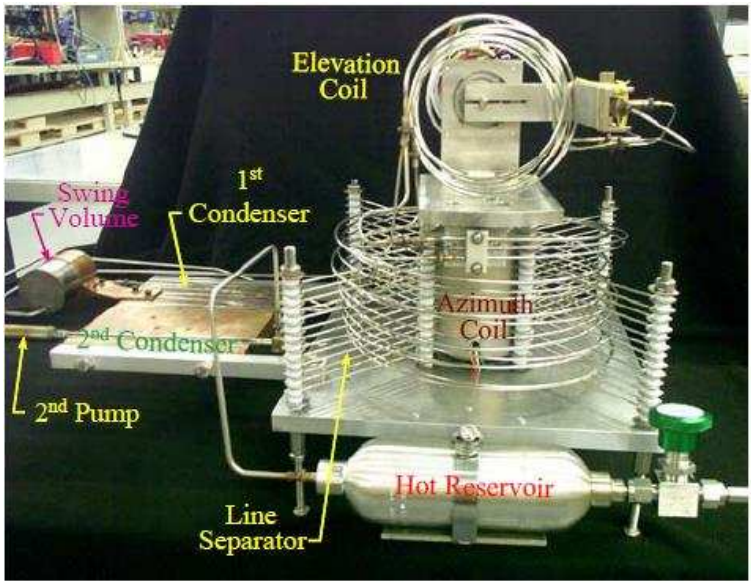

Fig.9 Detailed structure of across-gimbal N_2-CLHP[33]

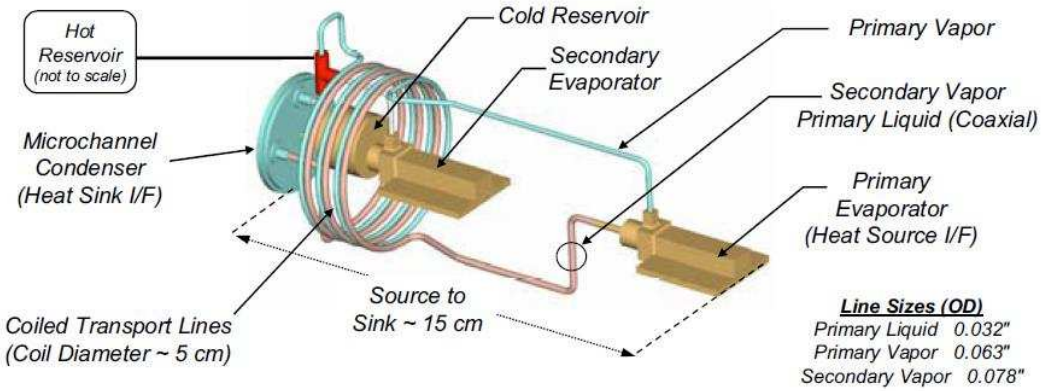

Fig.10 Detailed structure of short transport length Ne-CLHP[35]

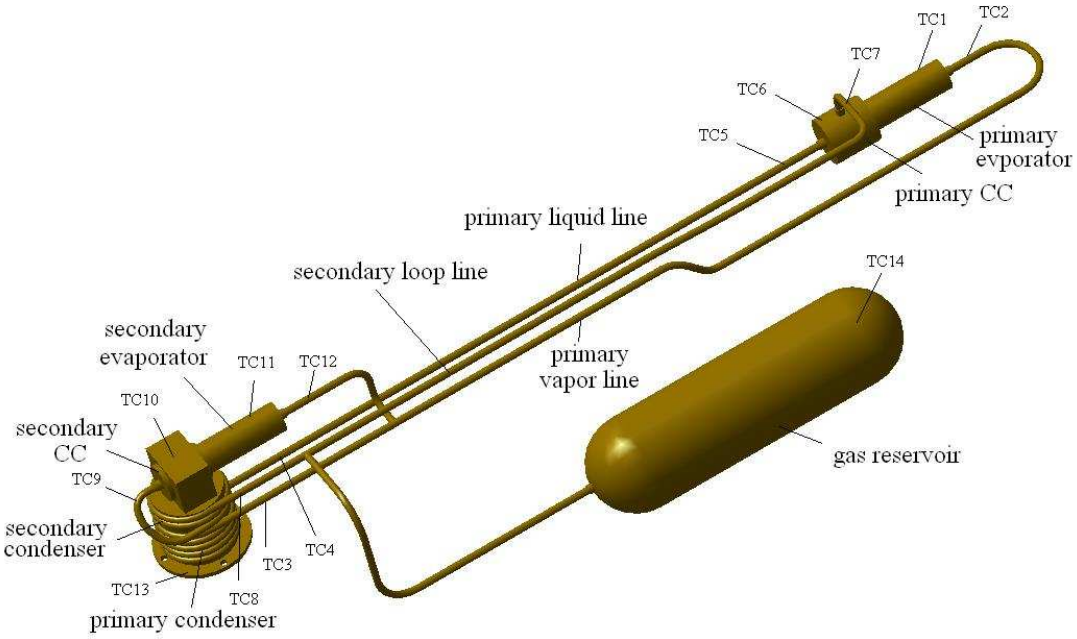

Fig.11 Detailed structure of N_2-CLHP with cylindrical condenser[41]

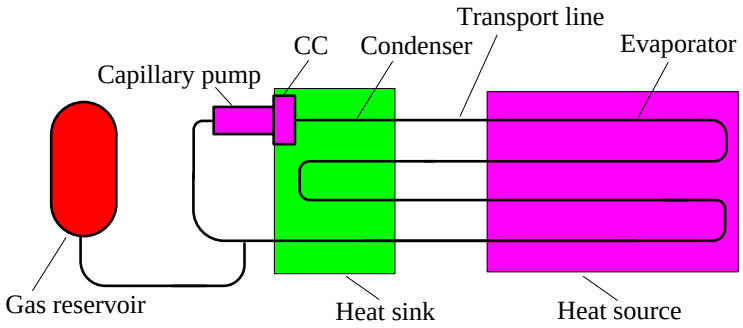

Fig.12 Schematic of the CLHP with type E

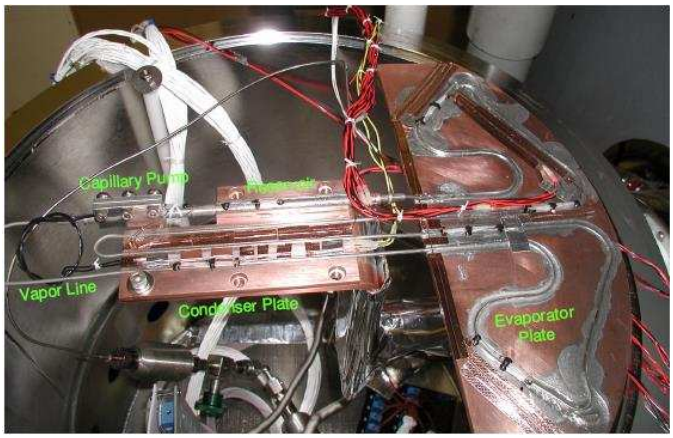

Fig.13 Detailed structure of the Ne-CLHP for large area cryocooling[62]